Baryon number fluctuations within the functional renormalization group approach

Wei-jie Fu

Dalian University of Technology

wjfu@dlut.edu.cn

The Third Symposium on Chiral Effective Field Theory, Oct. 28-Nov. 2, 2016

talk based on:
WF, J. M. Pawlowski, F. Rennecke, B.-J. Schaefer, arXiv:1608.04302 [hep-ph]
WF, J. M. Pawlowski, Phys.Rev.D 93,091501(R),2016
WF, J. M. Pawlowski, Phys.Rev.D 92,116006,2015

fQCD collaboration:
J. Braun, A. Cyrol, L. Fister, WF, T.K. Herbst, M. Mitter, N. Mueller,
J.M. Pawlowski, S. Rechenberger, F. Rennecke, N. Strodthoff

Outline

Introduction

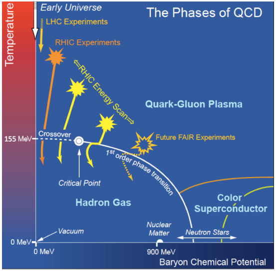

A sketch of QCD phase diagram, taken from *The Hot QCD White Paper, (2015), arXiv:1502.02730 [nucl-ex]*

Introduction

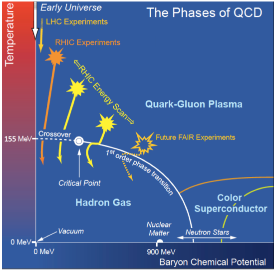

A sketch of QCD phase diagram, taken from *The Hot QCD White Paper, (2015), arXiv:1502.02730 [nucl-ex]*

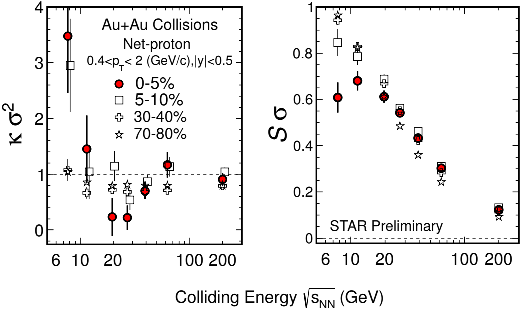

Kurtosis and skewness of net-proton distributions measured at RHIC, taken from *X. Luo (STAR), PoS CPOD2014, 019 (2014), arXiv:1503.02558 [nucl-ex]*

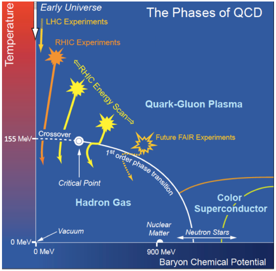

A sketch of QCD phase diagram, taken from *The Hot QCD White Paper, (2015), arXiv:1502.02730 [nucl-ex]*

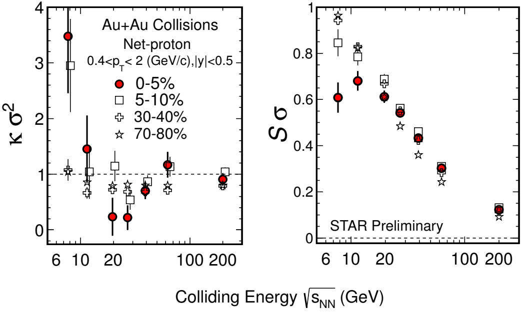

Kurtosis and skewness of net-proton distributions measured at RHIC, taken from *X. Luo (STAR), PoS CPOD2014, 019 (2014), arXiv:1503.02558 [nucl-ex]*

- The experimental programme should be accompanied by reliable theoretical predictions for the above observables and their relation to the CEP are highly demanded.

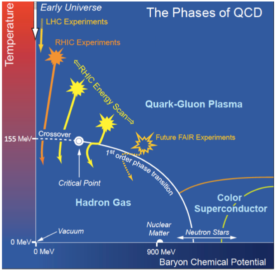

A sketch of QCD phase diagram, taken from *The Hot QCD White Paper, (2015), arXiv:1502.02730 [nucl-ex]*

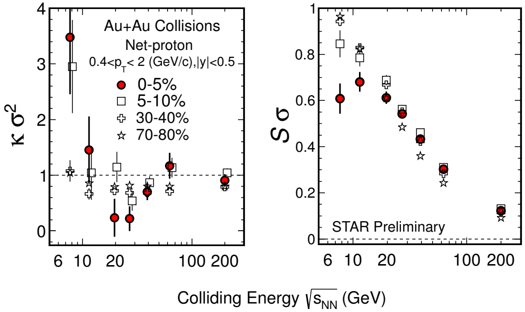

Kurtosis and skewness of net-proton distributions measured at RHIC, taken from *X. Luo (STAR), PoS CPOD2014, 019 (2014), arXiv:1503.02558 [nucl-ex]*

- The experimental programme should be accompanied by reliable theoretical predictions for the above observables and their relation to the CEP are highly demanded.
- In this talk, I will present our theoretical results, based on a QCD-improved low energy effective model.

Functional renormalization group

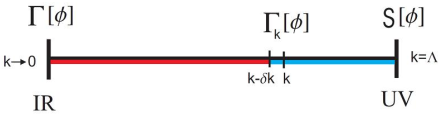

Effective action at RG-scale k

Functional renormalization group

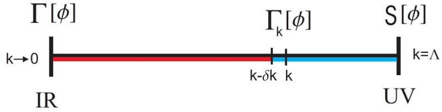

Effective action at RG-scale k

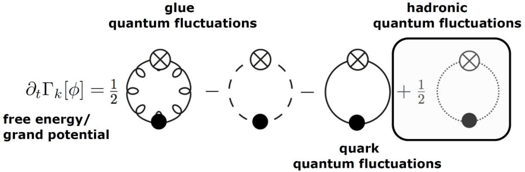

Functional renormalization group

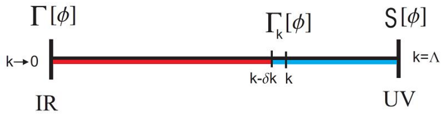

Effective action at RG-scale k

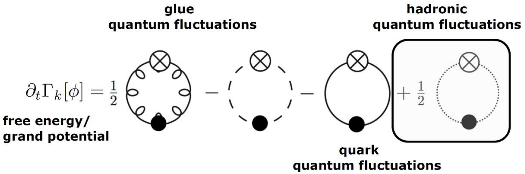

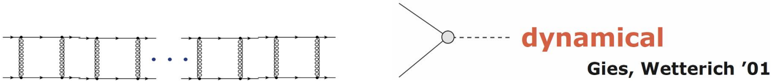

Dynamical hadronization

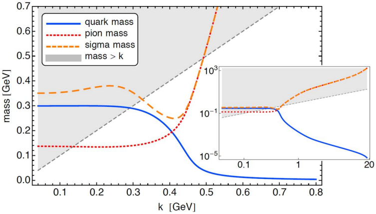

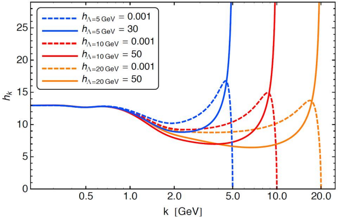

J. Braun, L. Fister, J. M. Pawlowski, F. Rennecke, PRD 94,034016 (2016), arXiv:1412.1045 [hep-ph]

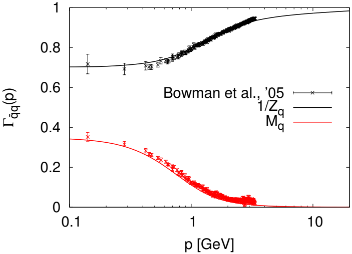

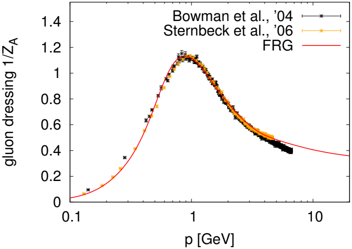

M. Mitter, J.M. Pawlowski, N. Strodthoff, PRD 91, 054035 (2015), arXiv:1411.7978 [hep-ph]

Low energy effective models and our truncations

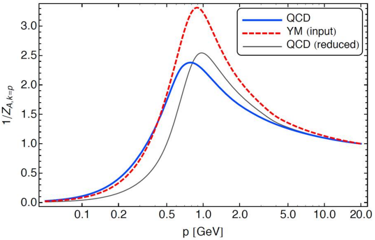

J. Braun, L. Fister, J. M. Pawlowski, F. Rennecke,

PRD 94,034016 (2016), arXiv:1412.1045 [hep-ph]

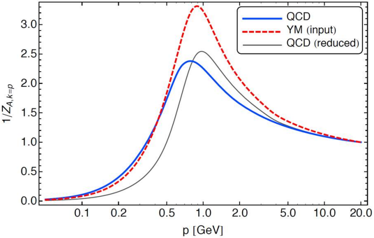

J. Braun, L. Fister, J. M. Pawlowski, F. Rennecke,

PRD 94,034016 (2016), arXiv:1412.1045 [hep-ph]

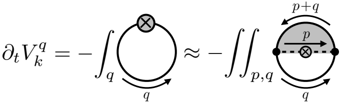

For the matter part, we use the following truncations:

$$\Gamma_k = \int_x \Big\{ Z_{q,k}\bar{q}(\gamma_\mu\partial_\mu - \gamma_0\mu)q + \frac{1}{2}Z_{\phi,k}(\partial_\mu\phi)^2$$

$$+ h_k\,\bar{q}\left(T^0\sigma + i\gamma_5\vec{T}\cdot\vec{\pi}\right)q + V_k(\rho) - c\sigma\Big\} + \cdots ,$$

Glue potential

the glue part is approximated as a QCD-enhanced glue potential with

$$V_{\rm glue}(L,\bar{L};t_{\rm glue}) = V_{\rm YM}(L,\bar{L};0.57\,t_{\rm glue})$$

a simple linear rescaling between Yang-Mills theory and QCD [*L.M. Haas, R. Stiele, J. Braun, J.M. Pawlowski, J. Schaffner-Bielich, 2013*]:

$$t_{\rm YM}(t_{\rm glue}) \approx 0.57\,t_{\rm glue}$$

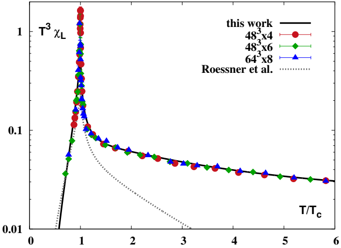

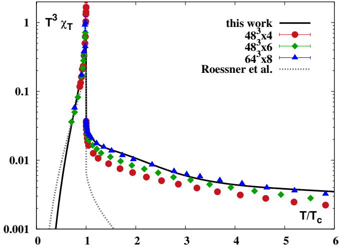

P.M. Lo, B. Friman, O. Kaczmarek, K. Redlich, C. Sasaki, PRD 88, 074502 (2013), arXiv:1307.5958 [hep-lat]

Thermodynamics

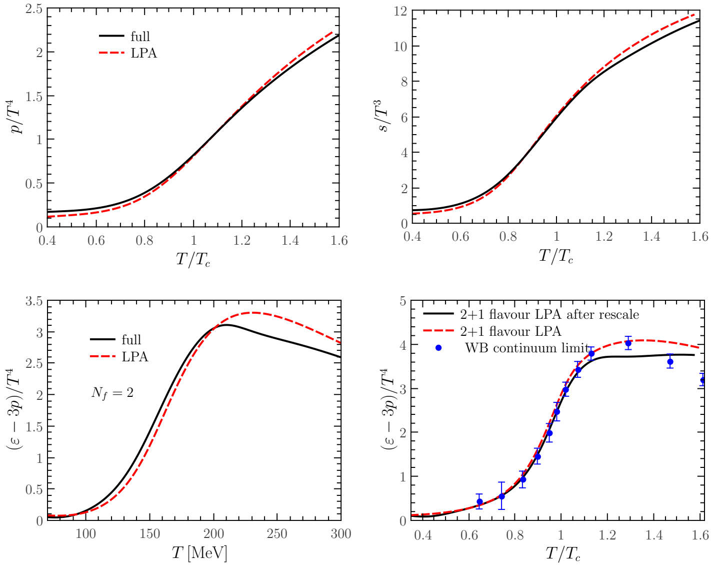

Baryon number fluctuations

The baryon number fluctuations are given by

$$\chi_n^{\mathrm{B}} = \frac{\partial^n}{\partial(\mu_{\mathrm{B}}/T)^n}\frac{p}{T^4}\,,$$

they are related with the cumulants of baryon multiplicity distributions by, such as

$$\begin{aligned} M &= VT^3\chi_1^{\mathrm{B}}, && \text{mean value} \\ \sigma^2 &= VT^3\chi_2^{\mathrm{B}}, && \text{variance} \\ S &= \chi_3^{\mathrm{B}}/(\chi_2^{\mathrm{B}}\sigma), && \text{skewness} \\ \kappa &= \chi_4^{\mathrm{B}}/(\chi_2^{\mathrm{B}}\sigma^2), && \text{kurtosis} \end{aligned}$$

Baryon number fluctuations

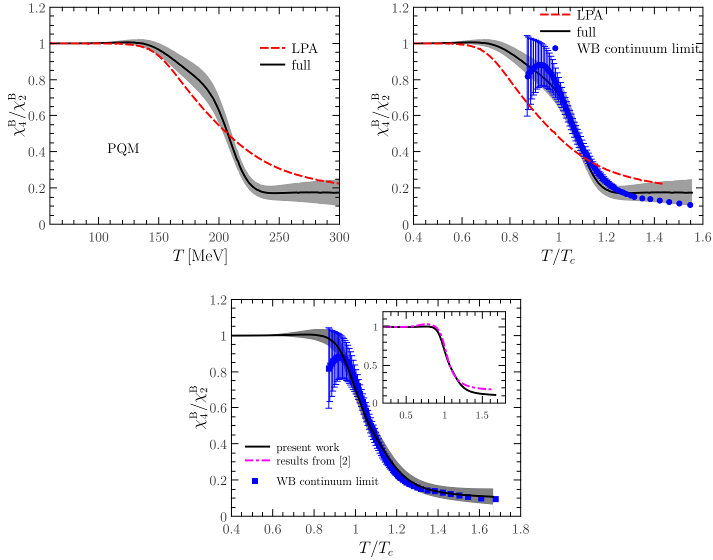

Freeze-out line

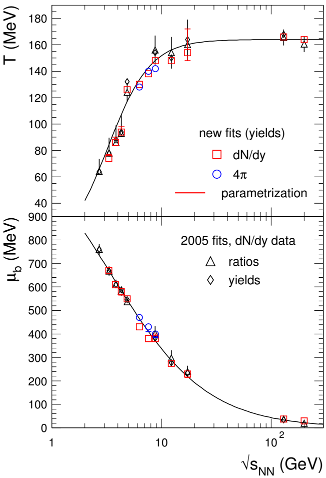

Freeze-out temperature and chemical potential obtained from the Statistical Hadronization Model, taken from [*A. Andronic, P. Braun-Munzinger, J. Stachel, (2009)*]

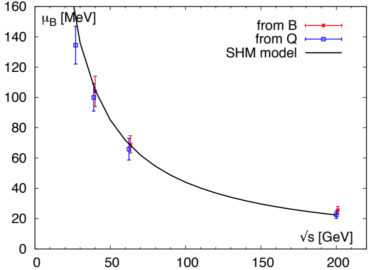

Freeze-out chemical potential obtained from lattice simulations, taken from [*S. Borsanyi et al. (2014)*]

Rescaling the chemical potential

For the chemical potential, we use the following linear rescale:

$$\mu_{B,N_f=2} = \frac{T_{c,N_f=2}(\mu_B = 0)}{T_{c,N_f=2+1}(\mu_B = 0)} \mu_{B,N_f=2+1} \,,$$

Rescaling the chemical potential

For the chemical potential, we use the following linear rescale:

$$\mu_{B,N_f=2} = \frac{T_{c,N_f=2}(\mu_B = 0)}{T_{c,N_f=2+1}(\mu_B = 0)} \mu_{B,N_f=2+1} \,,$$

with

$$T_{c,N_f=2+1}(\mu_B = 0) = 155\,\mathrm{MeV}$$

being the pseudo-critical temperature at $\mu_B = 0$ for flavour $N_f = 2+1$ from lattice simulations [*S. Borsanyi et al. (2010)*]. This temperature also agrees with the freeze-out temperature [*S. Borsanyi et al. (2014)*].

$$T_{c,N_f=2}(\mu_B = 0) = 180\,\mathrm{MeV}$$

is the pseudo-critical temperature at $\mu_B = 0$ in our calculation.

Rescaling the chemical potential

For the chemical potential, we use the following linear rescale:

$$\mu_{B,N_f=2} = \frac{T_{c,N_f=2}(\mu_B = 0)}{T_{c,N_f=2+1}(\mu_B = 0)} \mu_{B,N_f=2+1} \, ,$$

with

$$T_{c,N_f=2+1}(\mu_B = 0) = 155 \, \mathrm{MeV}$$

being the pseudo-critical temperature at $\mu_B = 0$ for flavour $N_f = 2 + 1$ from lattice simulations [*S. Borsanyi et al. (2010)*]. This temperature also agrees with the freeze-out temperature [*S. Borsanyi et al. (2014)*].

$$T_{c,N_f=2}(\mu_B = 0) = 180 \, \mathrm{MeV}$$

is the pseudo-critical temperature at $\mu_B = 0$ in our calculation.

$\sqrt{s}$ [GeV]	200	62.4	39	27	19.6	11.5	7.7
$\mu_{B,N_f=2}$ [MeV]	25.9	80.3	124.5	173.5	229.1	352.8	472.5

$\mu_{B,N_f=2}$ corresponding to different collision energy.

Correlating the skewness and kurtosis of baryon number distributions

We employ the skewness $S\sigma$ obtained in experiments to determine the freeze-out temperature in our calculations, then use this temperature to obtain the kurtosis $\kappa\sigma^2$ of the baryon number distributions.

Correlating the skewness and kurtosis of baryon number distributions

We employ the skewness $S\sigma$ obtained in experiments to determine the freeze-out temperature in our calculations, then use this temperature to obtain the kurtosis $\kappa\sigma^2$ of the baryon number distributions.

This approach is equivalent to inputing $S\sigma$ in our theoretical calculations, and then outputing $\kappa\sigma^2$, that can be compared with experimental results.

Correlating the skewness and kurtosis of baryon number distributions

We employ the skewness $S\sigma$ obtained in experiments to determine the freeze-out temperature in our calculations, then use this temperature to obtain the kurtosis $\kappa\sigma^2$ of the baryon number distributions.

This approach is equivalent to inputing $S\sigma$ in our theoretical calculations, and then outputing $\kappa\sigma^2$, that can be compared with experimental results.

In the same time, this approach correlates two important quantities of non-Gaussian distributions, and emphasise the relation between them.

Correlating the skewness and kurtosis of baryon number distributions

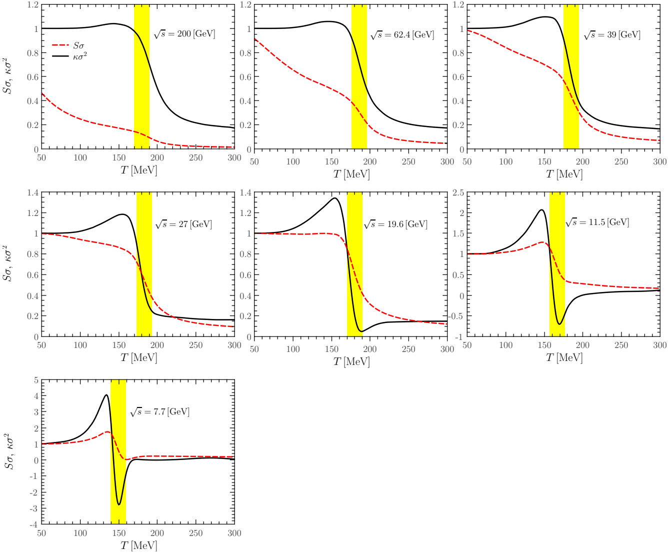

Effects of the full frequency dependence of the quark dispersion

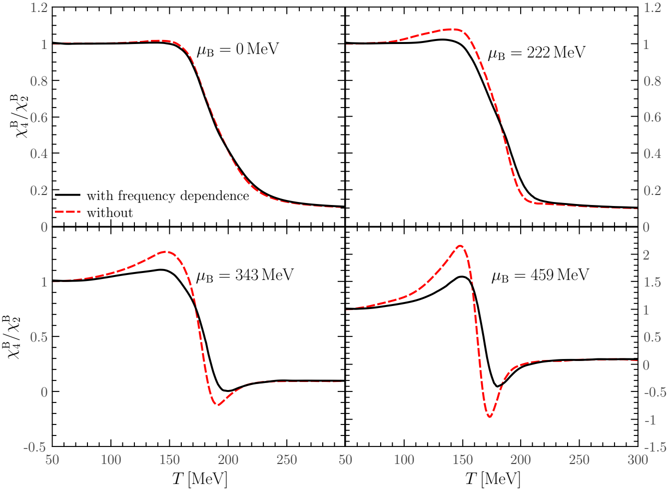

Comparison with experimental measurements

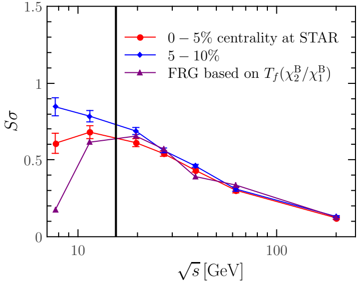

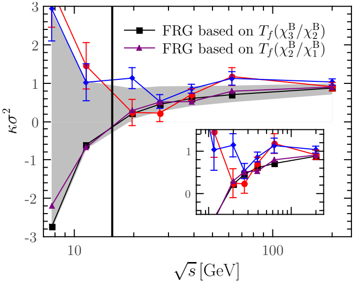

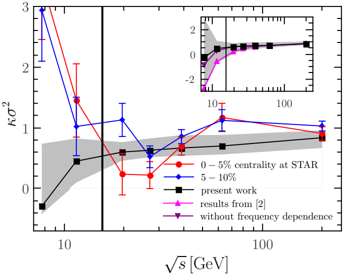

Summary and outlook

The improved truncations also leads to a better agreement with lattice simulations at vanishing chemical potential.

Summary and outlook

The improved truncations also leads to a better agreement with lattice simulations at vanishing chemical potential.

Our calculated results agree with the experimental measurements up to errors, for the colliding energy $\sqrt{s} \geq 19.6\,\mathrm{GeV}$.

Summary and outlook

The improved truncations also leads to a better agreement with lattice simulations at vanishing chemical potential.

Our calculated results agree with the experimental measurements up to errors, for the colliding energy $\sqrt{s} \geq 19.6\,\mathrm{GeV}$.

An obvious discrepancy, between the theory and experiment, develops when the colliding energy is less than $19.6\,\mathrm{GeV}$.

Summary and outlook

Dynamical hadronization and glue fluctuations are indispensable to push up the initial scale of flows.

Summary and outlook

Dynamical hadronization and glue fluctuations are indispensable to push up the initial scale of flows.

We are working in this direction.

Thank you for your attentions!

Thermodynamics: quark-meson model

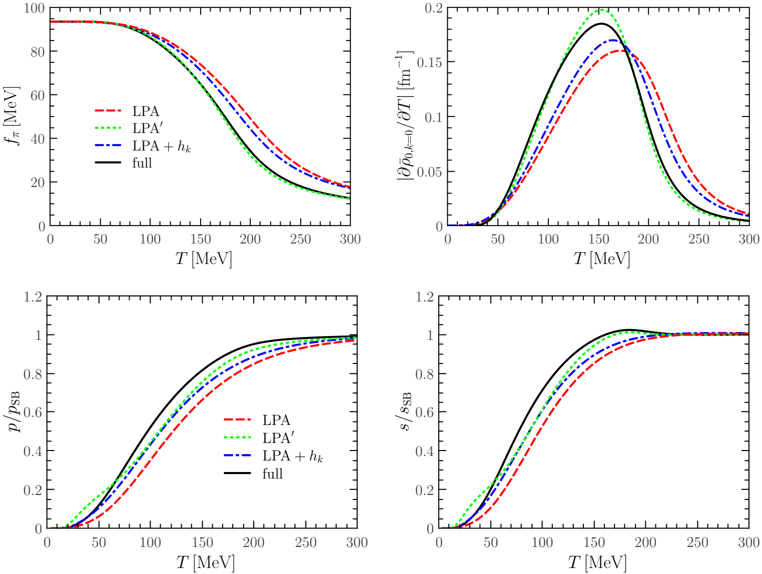

Baryon number fluctuations: quark-meson model

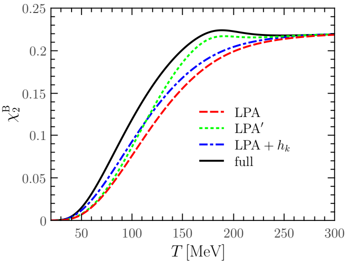

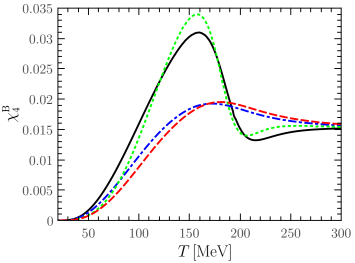

Baryon number fluctuations: quark-meson model

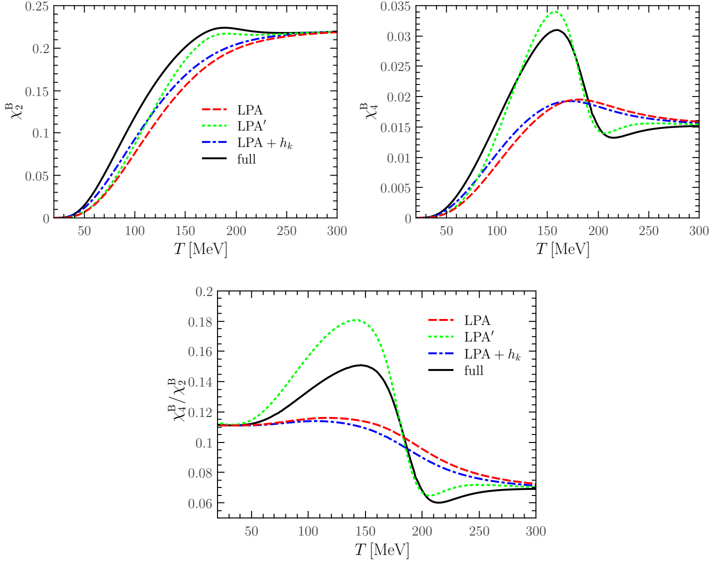

Baryon number fluctuations: QCD-enhanced Polyakov–quark-meson model

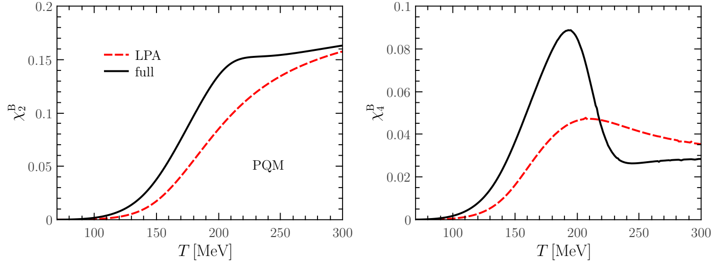

Baryon number fluctuations: QCD-enhanced Polyakov–quark-meson model